Cell Mol Neurobiol (2013) 33:443–452
DOI 10.1007/s10571-013-9911-1

ORIGINAL RESEARCH

A Novel Domain of Amino-Nogo-A Protects HT22 Cells Exposed to Oxygen Glucose Deprivation by Inhibiting NADPH Oxidase Activity

Fan Guo · Huiwen Wang · Liya Li · Heng Zhou · Haidong Wei · Weilin Jin · Qiang Wang · Lize Xiong

Received: 10 September 2012 / Accepted: 16 January 2013 / Published online: 26 January 2013

Abstract This study aimed to investigate the protective effect of the M9 region (residues 290–562) of amino-Nogo-A fused to the human immunodeficiency virus trans-activator TAT in an in vitro model of ischemia–reperfusion induced by oxygen–glucose deprivation (OGD) in HT22 hippocampal neurons, and to investigate the role of NADPH oxidase in this protection. Transduction of TAT-M9 was analyzed by immunofluorescence staining and western blot. The biologic activity of TAT-M9 was assessed by its effects against OGD-induced HT22 cell damage, compared with a mutant M9 fusion protein or vehicle. Cellular viability and lactate dehydrogenase (LDH) release were assessed. Neuronal apoptosis was evaluated by flow cytometry. The Bax/Bcl-2 ratio was determined by western blotting. Reactive oxygen species (ROS) levels and NADPH oxidase activity were also measured in the presence or absence of an inhibitor or activator of NADPH oxidase. Our results confirmed the delivery of the protein into HT22 cells by immunofluorescence and western blot. Addition of 0.4 μmol/L TAT-M9 to the culture medium effectively improved neuronal cell viability and reduced LDH release induced by OGD. The fusion protein also protected HT22 cells from apoptosis, suppressed overexpression of Bax, and inhibited the reduction in Bcl-2 expression. Furthermore, TAT-M9, as well as apocynin, decreased NADPH oxidase activity and ROS content. The protective effects of the TAT-M9 were reversed by TBCA, an agonist of NADPH oxidase. In conclusion, TAT-M9 could be successfully transduced into HT22 cells, and protected HT22 cells against OGD damage by inhibiting NADPH oxidase-mediated oxidative stress. These findings suggest that the TAT-M9 protein may be an efficient therapeutic agent for neuroprotection.

Keywords Nogo-A · Oxygen and glucose deprivation · Oxidative stress · Apoptosis · NADPH oxidase

Introduction

Stroke is the second most common cause of death and the leading cause of serious disability in adults in the world. Oxygen–glucose deprivation (OGD) has been implicated in the neuronal cell death in disorders such as ischemia and Alzheimer's disease (Albrecht et al. 2005), and has been shown to produce some of the metabolic aspects of stroke injury in vitro leading to neuronal insult (Taylor et al. 1995; Fordel et al. 2007). Thus, OGD models have been widely used to investigate the pathology and pharmacology of ischemic injury. The pathogenesis of cerebral ischemic injury is complex and incompletely understood. However, overproduction of reactive oxygen species (ROS) during and after ischemia plays an important role in the development of oxidative stress following ischemic injury. Elevated levels of ROS disturb neuronal function, which could activate apoptotic pathways and lead to neuronal damage (Valko et al. 2007). Reduction of oxidative stress

Fan Guo and Huiwen Wang contributed equally to this work.

F. Guo · H. Wang · L. Li · H. Zhou · H. Wei · Q. Wang (✉) · L. Xiong (✉)
Department of Anesthesiology, Xijing Hospital, Fourth Military Medical University, Xi'an 710032, Shaanxi, China
e-mail: wangqiang@fmmu.edu.cn

L. Xiong
e-mail: mzkxlz@163.com

W. Jin
Institute of Neurosciences, School of Life Sciences and Biotechnology, Shanghai Jiao Tong University, Shanghai 200240, China

is considered a promising target for attenuating the neuronal damage following ischemia.

Among free radical-producing enzyme systems, NADPH oxidase 2 is widely expressed in the central nervous system and its activation plays a major role in stroke-induced oxidative injury. NADPH oxidase is activated after ischemia, and inhibition of NADPH oxidase attenuated oxidative injury (Yoshioka et al. 2011; Chen et al. 2009; Miller et al. 2006). These findings indicate an important role of NADPH oxdiase in neuronal damage following ischemic injury.

Nogo-A is a myelin-associated neurite inhibitory factor. It has been shown to inhibit the outgrowth of axonal processes after central nervous system injury. However, the function of neuronal Nogo-A is still widely uncharacterized. Inhibition of Nogo-A enhanced axonal sprouting and helped neurologic recovery in rodents with ischemic injury (Papadopoulos et al. 2002; Seymour et al. 2005). On the other hand, recent studies have shown that the expression of Nogo-A changes after the onset of stroke, decreasing in the early stages, then increasing in the long term (Cheatwood et al. 2008). Moreover, amino-Nogo-A, a long specific region (amino acids 186–1,004) of Nogo-A, showed a strong cytoprotective effect against H_2O_2-induced oxidative stress in vitro, and the M9 region (residues 290–562) may be the pivotal domain for these protective effects (Mi et al. 2012). Taken together with other results (Kilic et al. 2010), these findings indicate that Nogo-A may play a survival-promoting role in the early phase after ischemic injury, and that interruption of Nogo-A function at different time points could lead to various effects. However, the neuroprotective effects of M9 in OGD-induced cell insult are still unclear.

In this study, we used the HIV TAT trans-activator gene product fused to M9 protein (TAT-M9) to form an agent that could cross the cell membrane. We also examined whether TAT-M9 had a protective effect against OGD-induced neuronal cell injury in HT22 cells. In addition, we explored whether NADPH oxidase was involved in the neuroprotective effect of TAT-M9.

Materials and Methods

Construction, Purification, and Transduction of TAT-M9 Fusion Proteins

TAT-M9 was constructed and purified as described by Mi et al. (2012). Briefly, the coding sequences of M9 (aa290–562) and M9CA (M9 cysteine residues at positions 424, 464, and 559 were mutated into alanine) were amplified by LA-PCR and subcloned into pTAT-HA expression vector. All constructs were then inserted in vector pTAT-HA in fusion with the 6×His, TAT protein transduction domain and HA Tag. Fusion protein was purified by Ni–NTA-agarose chromatography (Merck, Darmstadt, Germany). The size and purity of all proteins were confirmed by sodium dodecyl sulfate–polyacrylamide gel electrophoresis (SDS-PAGE). After dialysis and filtration, the proteins were subpackaged and stored at −80 °C.

For the delivery of TAT fusion proteins into cells, 0.4 μmol/L TAT-M9 protein was added to the cell culture medium for 1 h (the concentrations and time courses were used in pre-experiments) and the transducible effect of TAT fusion protein was analyzed by immunofluorescence using an anti-6×His antibody. The fusion protein TAT-M9CA, in which the cysteine residues at positions 424, 464, and 559 were mutated into alanine, was also constructed. HT22 cells were incubated with this fusion protein by the same procedure for the purpose of comparisons with TAT-M9. Transducible effect of TAT fusion proteins was also analyzed by western blotting with anti-6×His antibody.

Cell Culture

The HT22 cells were cultured in commercial high glucose Dulbecco's modified Eagle's medium supplemented with 10 % (volume/volume) heat-inactivated fetal bovine serum, 100 U/mL penicillin, and 100 μg/mL streptomycin as normal condition. They were maintained at 37 °C in a 5 % CO_2/air environment using uncoated T-75 Falcons. For the experiments, the cells were treated as described below.

OGD Model

For HT22 cells exposed to OGD, the culture media were changed to a deoxygenated glucose-free or an oxygenated glucose-containing (for controls) Earle's balanced salt solution at pH 7.4. Then, the cells were transferred to a sealed hypoxic box containing a mixture of 95 % N_2 and 5 % CO_2 at 37 °C, or normal culture conditions for 2 h. Following OGD exposure, the HT22 cells were reoxygenated by high glucose DMEM without serum for 22 h. TAT-M9 or TAT-M9CA was added into the medium through the OGD and reoxygenated (OGD/R) procedure at different concentrations as described below. Tetrabromocinnamic acid (TBCA; EMD Chemicals, Gibbstown, NJ), which is a highly specific CK2 inhibitor, has been shown to activate NADPH oxidase (Kim et al. 2009). TBCA (10 μmol/L) was added to the medium 30 min before and during OGD/R. Fifty percent DMSO in PBS was used as a vehicle (Kim et al. 2009). Apocynin (100 μmol/L) was added to the medium during OGD/R (Nagasawa et al. 2007).

Assessment of Cell Viability and Cell Death

During OGD/R, the HT22 cells were co-cultured in normal medium, vehicle, or in the absence or presence of TAT-M9 or TAT-M9CA at different concentrations of 0.1, 0.2, and 0.4 μmol. Following OGD/R, cell viability was evaluated by MTT assay as described previously (Gou et al. 2011). In brief, MTT solution (5 mg/mL in DMEM) was added to the medium and the cells were incubated for 4 h at 37 °C. After the medium had been removed, the cell and dye crystals were solubilized by adding 200 μL of dimethylsulfoxide (DMSO), and the absorption at 570 nm was measured using a Model 550-microplate reader (Bio-Rad Lab, CA, USA). The cell relative viability was calculated using the OD_{570} value for each group as a percent of the mean OD_{570} value for the control group and repeated for five times.

Measurement of Lactate Dehydrogenase (LDH) Release

During the OGD/R procedure, the HT22 cells were co-cultured in normal medium or in the absence or presence of TAT-M9, TAT-M9CA, or vehicle at concentrations of 0.4 μmol. A colorimetric assay kit (LDH; Nanjing Jiancheng, China) for the quantification of cell death was performed as previously described (Gou et al. 2011), based on measurement of the activity of LDH released from the cytosol of damaged cells into the supernatant. It was also used to assess glucose cytotoxicity. The activity unit was defined as units per deciliter and the test was repeated for five times.

Flow Cytometry Analysis for Cell Apoptosis

Apoptosis was assessed using an apoptosis detection kit. Briefly, cells were collected after treatment, washed twice in ice-cold PBS, and resuspended in binding buffer at a density of 1×10^6 cells/mL. Cells were incubated simultaneously with fluorescein-labeled annexin V and propidium iodide (PI) for 20 min and analyzed by flow cytometry. Annexin V-FITC-generated signals were detected using an FITC signal detector (FL1, 525 nm). PI signals were monitored using a detector reserved for phycoerythrin emission (FL2, 575 nm). The test was repeated for three times and data were analyzed using Cell Quest software from BD.

Western Blot Analysis

After different treatments, HT22 cells from different groups were collected and lysed with modified RIPA-buffer supplemented with a protease inhibitor-cocktail and 100 μmol phenylmethanesulfonyl fluoride on ice for 30 min. After 20-min centrifugation, the total proteins concentration was quantified using a BCA kit. Equal amounts of total protein lysates were subjected to 12 % sodium dodecyl SDS-PAGE and transferred onto polyvinylidene difluoride membranes (Millipore Corp.). After blocking with 3 % BSA, the membranes were incubated with primary antibodies (Bcl-2, 1:200; Bax, 1:1000; $gp91^{phox}$ 1:1000; $p47^{phox}$, 1:1000; 6×His, 1:400; Abcam, USA) in phosphate-buffered saline (PBS) 0.1 % Tween-20 overnight at 4 °C. The membranes were then incubated with horseradish peroxidase-conjugated anti-rabbit immunoglobulin G at a 1:10,000 dilution (KangWei Inc. China.). Immunoreactive proteins were then visualized by enhanced chemiluminescence. The signals were quantified by densitometry using a western blotting detection system (Alpha Innotech, USA). GAPDH or tublin (KangWei Inc. China) served as the loading control.

Immunofluorescence

Immunofluoresence staining was performed according to the standard protocol. For analysis of TAT protein transfusion, after treatments, samples were washed with PBS and 4 % paraformaldehyde, permeabilized with 0.1 % Triton-X-100, washed three times for 5 min each in PBS, and immersed for 30 min in PBS containing 0.3 % Triton X-100 and 10 % normal goat serum. After three further rinses in PBS, sections were incubated overnight at 4 °C with a specific 6×His antibody (1:200, Abcam, USA) dissolved in PBS containing 0.3 % Triton X-100 and 2 % normal goat serum. Then, the sections were incubated in FITC-labeled secondary antibody solution (1:500, Sigma, USA) for 1 h at room temperature. The two incubation steps were followed by three washes with PBS (10 min each time). Images were captured using a Model BX-60 fluorescence microscope (Olympus Corporation, Tokyo, Japan).

Measurement of ROS Levels

As described previously (Mi et al. 2012), the cell penetrative dihydroethidium (DHE) was used to assess real-time formation of superoxide in HT22 neurons following the provided protocol (Beyotime company, China). DHE in DMSO was added directly to the culture media at final concentration of 10 μM and incubated at 37 °C for 30 min. Then, the neurons were rinsed once rapidly in PBS and immediately observed under a fluorescence microscope (Leica DMI6000B, Leica Microsystems GmbH, Wetzlar, Germany) with excitation of 488 nm and emission of 525 nm, and were analyzed by Image Pro-Plus software (IPP 6.0, MediaCybernetics, Silver Spring, MD, USA).

Statistical Analysis

SPSS 11.0 for Windows software (SPSS Inc, Chicago, IL) was used to conduct statistical analyses. Values are

presented as mean ± SEM. Results were compared by one-way analysis of variance. Between-group differences were assessed by the post hoc Student–Newman–Keuls test. Values of $P \leq 0.05$ were considered statistically significant.

Results

Transduction of TAT-M9 Fusion Protein into HT22 Cells

According to former studies, the M9 domain of Nogo-A comprises amino acids 290–562 (Fig. 1a). M9 fused to TAT was constructed and purified (Fig. 1b). Western blotting results proved TAT-M9 and TAT-M9CA transduced into HT22 cells 1 h after efficiently (Fig. 1c) and sustained stable. Immunofluorescence staining was used to confirm the intracellular delivery of TAT-M9 into HT22 cells. A rabbit anti-6×His antibody revealed that TAT-M9 was transduced into cells, while fluorescence signals were absent in cells treated with vehicle (PBS). In addition, the same fluorescence signals were detected in HT22 cells treated with TAT-M9CA (Fig. 1d).

TAT-M9 Increases Cell Viability and Prevents LDH Release in HT22 Cells Exposed to OGD

The viability of HT22 cells was markedly decreased after OGD insult compared with the control group. Treatment of cells with TAT-M9 at a concentration of 0.4 μmol significantly increased the viability of HT22 cells exposed to OGD. However, the same concentration of TAT-M9CA or vehicle was not able to increase the viability of HT22 cells exposed to OGD (Fig. 2a). Exposure of HT22 cells to OGD for 2 h followed by 22 h of restoration produced an obvious elevation of LDH activity in the culture supernatant compared with that of sham cells (Fig. 2b). The elevation of LDH induced by OGD was markedly attenuated by the addition of 0.4 μmol of TAT-M9. On the other hand, TAT-M9CA or vehicle did not effectively prevent the rise in LDH activity in the culture supernatant following OGD.

TAT-M9 Inhibits Cellular Apoptosis in HT22 Cells Exposed to OGD

Annexin/PI co-staining and flow cytometry were used to study the extent of apoptosis in OGD-exposed neuronal cultures. A representative result of flow cytometry was presented in Fig. 3a–d. The lower right quadrant represented the percentage of early apoptotic cells, while the upper right quadrant depicted the percentage of late apoptotic cells and dead cells. We analyzed the lower right quadrant for the apoptotic cells. In untreated control cultures, there was only a very low level of apoptosis (Fig. 3a). After 2 h of OGD and 22 h of reoxygenation, the percentage of apoptotic neurons rose from 5.1 to 38.6 % (Fig. 3b). Treatment with 0.4 μmol TAT-M9 resulted in a significant reduction in the numbers of apoptotic neurons following OGD to 7.4 % (Fig. 3c). TAT-M9CA showed no such effect with 39.3 % of neurons showing signs of apoptosis (Fig. 3d). The experiment was repeated three times (Fig. 3e).

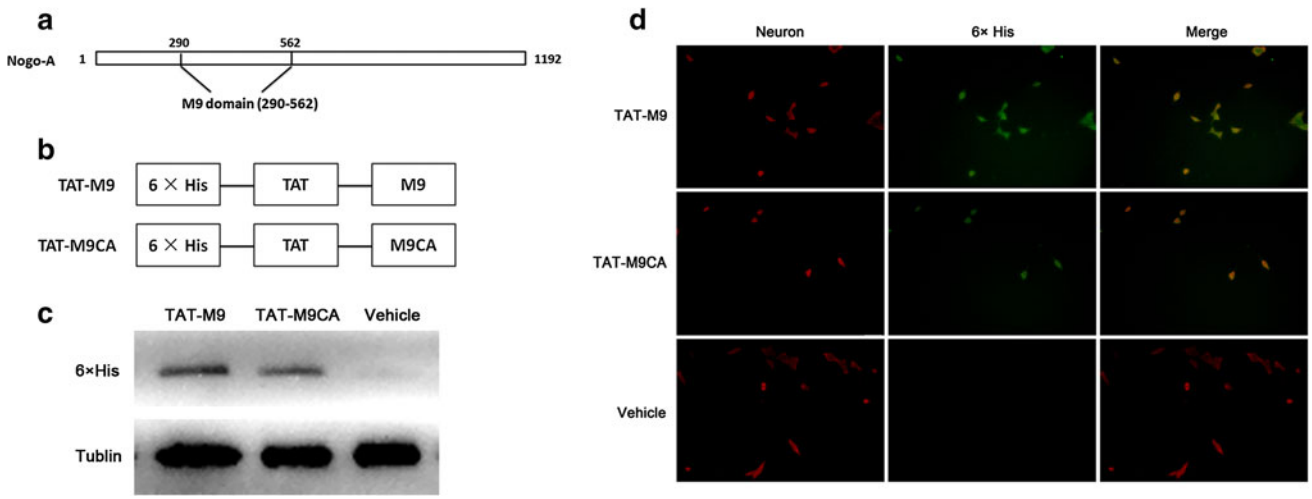

Fig. 1 Structure and construction of TAT-M9, and transduction into HT22 cells. **a** The structure of the M9 domain from Nogo-A. **b** The construction of TAT-M9CA and TAT-M9. **c** HT22 cells were cultured in the presence of TAT-M9, TAT-M9CA, or vehicle for 1 h and then tested by western blotting with anti-6×His primary antibody. **d** Representative immunofluorescence staining also showed HT22 cells treated with TAT-M9, vehicle, or TAT-M9CA

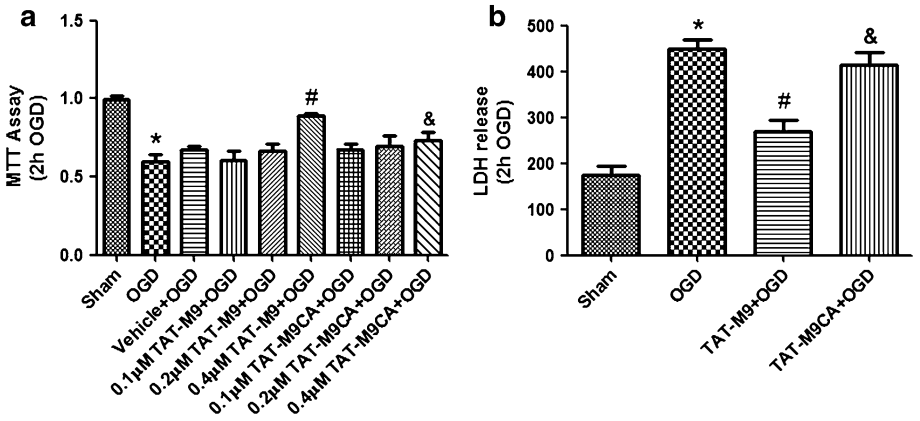

Fig. 2 Effect of TAT-M9 on cell viability and LDH release in HT22 cells exposed to OGD. **a** An MTT test was used to assess the effect of TAT-M9 on cell viability. **b** Effects of TAT-M9 on OGD-induced LDH release. The LDH activity in the culture medium was determined by a commercially available assay. Exposure of HT22 cells to OGD showed an obvious elevation of LDH release compared with the sham group, while LDH was markedly attenuated by TAT-M9 treatment, but not TAT-M9CA treatment. Values are expressed as mean ± SEM; $n = 5$ per group. $^{*}P < 0.05$ versus Sham group, $^{\#}P < 0.05$ versus OGD group, $^{\&}P < 0.05$ versus TAT-M9 group

TAT-M9 Ameliorates the Bax/Bcl-2 Ratio in HT22 Cells Exposed to OGD

Bcl-2 and Bax belong to the Bcl-2 family of proteins that promote cell survival, whereas Bax accelerates apoptosis. Western blotting results revealed that Bax expression was significantly increased in the OGD group compared with the sham group. Addition of TAT-M9 at a concentration of 0.4 μmol decreased the Bax expression level. On the other hand, the level of Bcl-2 in the OGD group was significantly decreased compared with the control group, but recovered following TAT-M9 treatment (Fig. 4). Statistical analysis of the Bax/Bcl-2 ratio revealed that TAT-M9 treatment could ameliorate the OGD-induced elevation in Bax/Bcl-2 ratio in HT22 cells, while TAT-M9CA and vehicle showed no such effects.

TAT-M9 Protects HT22 Cells Exposed to OGD via Suppression of NADPH Oxidase

TAT-M9, as well as apocynin, could efficiently inhibit the increase in total $gp91^{phox}$ and $p47^{phox}$ protein levels in cells with OGD-induced damage, improve cell viability and reduce LDH release. A recently developed agonist of NADPH oxidase, TBCA, reversed the protective effect of TAT-M9. In contrast, neither PBS nor DMSO could reverse the protective effect of TAT-M9 (Fig. 5).

TAT-M9 Reduces ROS Production in HT22 Cells Exposed to OGD

Following OGD, abundant ROS were generated and the production of ROS could initiate a series of signaling pathways. Compared with the sham group, the OGD group showed increased total ROS production. In contrast, treatment with TAT-M9 or apocynin significantly reduced the increase in total ROS generation. However, this protective effect of TAT-M9 could be reversed by TBCA (Fig. 6).

Discussion

Stroke is one of the leading cause of death and disability in the world. Ischemia and reperfusion causes significant cell damage because of the insufficient supply of glucose and oxygen. To better understand the mechanisms underlying neuronal cell injury and potential protective agents, OGD/R is commonly used to simulate cerebral ischemia reperfusion injury models in vitro. In the present study, we aimed to examine the effect of a novel region of Nogo-A, M9, on OGD/R injury in HT22 cells.

TAT protein has good potential for disease therapy based on its ability to deliver full-length proteins and peptides through plasma membranes and into cells. Indeed, various TAT fusion proteins are able to transduce cells in vitro and in vivo (Katsura et al. 2008; Nagel et al. 2008; Kilic et al. 2003; Gou et al. 2011; Wang et al. 2008). In the present study, the M9 region of Nogo-A (residues 290–592) was fused to the HIV-TAT protein as previously described (Mi et al. 2012). We proved that this novel protein could be efficiently delivered into HT22 cells when added to the culture medium. Then, we found that 0.4 μmol/L TAT-M9 in culture medium could increase the viability and suppress the OGD-induced increase in LDH release compared with that in cultures exposed to OGD alone. Meanwhile, the same concentration of TAT-M9CA did not attenuate OGD-induced damage in HT22 cells. On the other hand, 0.4 μmol/L TAT-M9 or TAT-M9CA did not interrupt normal cell growth in the absence of OGD damage. Those

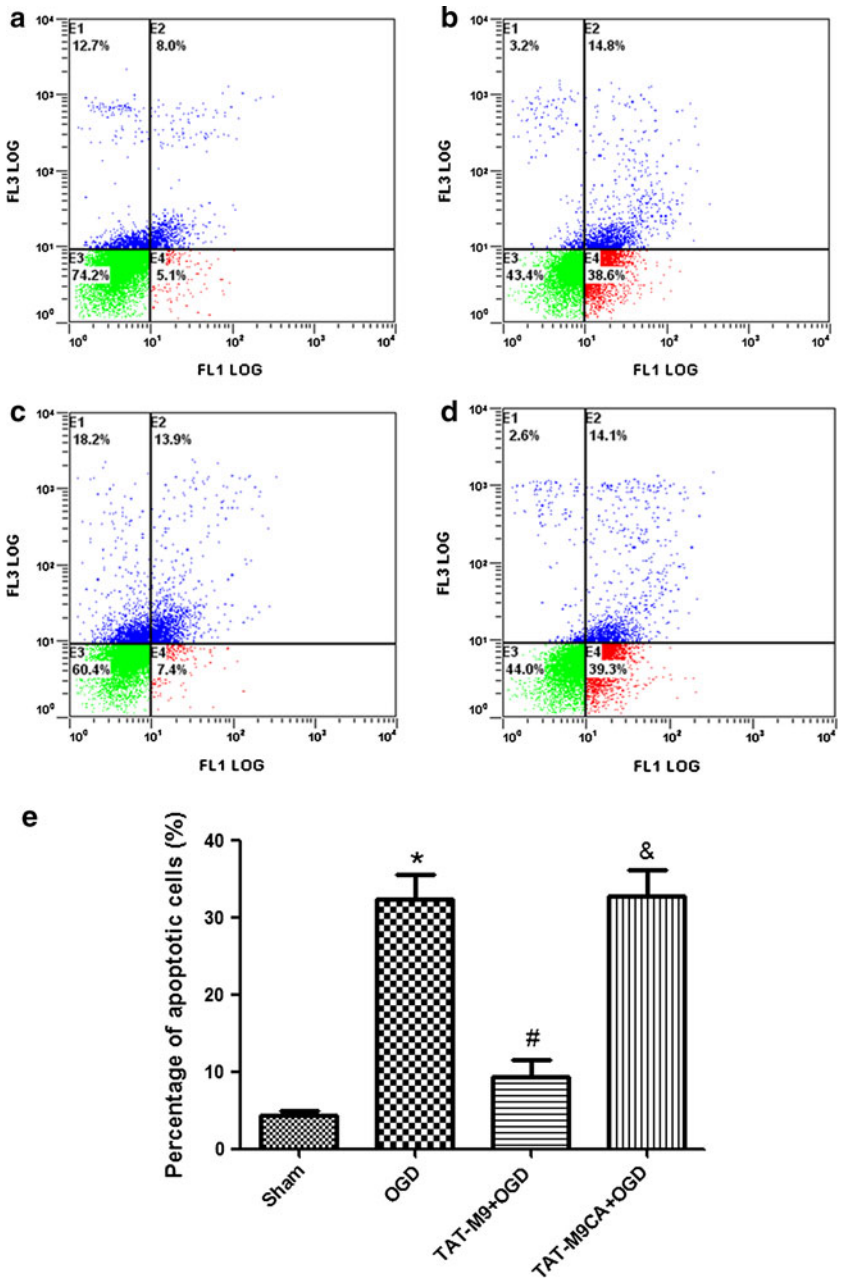

Fig. 3 Effects of TAT-M9 on cellular apoptosis in HT22 cells exposed to OGD. **a**–**d** Flow cytometry profiles following annexin/PI staining of **a** control neuronal cultures, **b** cultures treated with 2 h of OGD and 22 h of reoxygenation, **c**, **d** cultures treated with 2 h of OGD and 22 h of reoxygenation in the presence of 0.4 μmol TAT-M9 or TAT-M9CA, respectively. The experiment was repeated three times and the percentage of apoptotic cells for each group was shown (**e**). $^{*}P < 0.05$ versus Sham group, $^{\#}P < 0.05$ versus OGD group, $^{\&}P < 0.05$ versus TAT-M9 group

finding indicated that TAT-M9 had a protective effect against OGD-induced damage in HT22 cells.

Apoptosis, also known as programed cell death, can be triggered by numerous mediators including oxidative stress resulting from ischemia–reperfusion injury (Krantic et al. 2007). In the current study, apoptosis was measured by flow cytometry, which precisely quantifies apoptosis by PI and annexin V dual staining. The early phase of apoptosis was represented by annexin+/PI− cells, and these neurons are important for proper treatment as a "last save." The number of annexin+/PI− cells markedly increased after OGD/R. TAT-M9 could efficiently reduce the early phase of apoptosis, but TAT-M9CA could not. However, the percentage of cells in the late phase of apoptosis and undergoing necrosis (annexin+/PI+) were not significantly different among groups, except for the Sham group. This result, together with the MTT and LDH results mentioned above, indicated that the protective effect of TAT-M9 against HT22 cell injury was mostly due to an effect on apoptosis rather than necrosis.

Bcl-2 family proteins, including pro-apoptotic (Bax, Bad) and anti-apoptotic (Bcl-2, Bcl-xL) proteins, play a crucial role in the process of apoptosis (Susnow et al. 2009). In the current study, TAT-M9 treatment could decrease cell apoptosis by decreasing the Bax/Bcl-2 ratio. By suppressing both the overexpression of Bax and

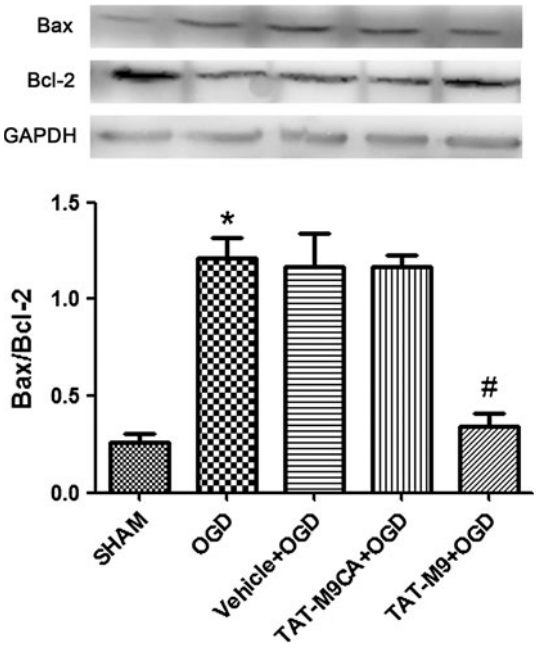

Fig. 4 Effects of TAT-M9 on Bax and Bcl-2 expression in HT22 cells exposed to OGD Effects of TAT-M9 on Bax and Bcl-2 protein expression. Statistical analysis of the Bax/Bcl-2 ratio. Values are expressed as mean ± SEM; $n = 3$ per group. $^{*}P < 0.05$ versus Sham group, $^{\#}P < 0.05$ versus OGD group

downregulation of Bcl-2 induced by OGD, TAT-M9 modulates the Bax/Bcl-2 equilibrium to suppress the drive toward apoptosis induced by OGD. However, it remains to be established whether other apoptosis-related signaling pathways are involved in the protective effects of TAT-M9.

Previous studies have shown that ROS plays a critical role in cellular functions including proliferation and differentiation, as well as processes such as apoptosis (Kemp et al. 2008). On one hand, proper reactivation of ROS is important and necessary for maintaining basic molecular function. On the other hand, prolonged increases of ROS could be risky for the body. OGD could cause massive generation of ROS, and these might target neuronal cells, which are particularly vulnerable. NADPH oxidase is considered to be a major source of ROS in many physiologic and pathological processes (Chrissobolis and Faraci. 2008; Bedard and Krause 2007). In our preliminary experiments, we proved that extracellular signal regulated protein kinases (ERK1/2) increased in TAT-M9-treated group and ERK1/2 activation was related to activation of NADPH oxidase (Kilic et al. 2010; Yoo et al. 2005). For these reasons, we assumed that TAT-M9 might suppress the activity of NADPH oxidase and thereby alter ROS production.

NADPH oxidase is a multiunit enzyme composed of membrane-bound subunits including $gp91^{phox}$ and cytoplasmic subunits including $p47^{phox}$ (Anthony et al. 1997). Expression of $gp91^{phox}$ and $p47^{phox}$, important catalytic subunits of NADPH oxidase, has been shown to be up-regulated in ischemic stroke (Walder et al. 1997). Thus, we confirmed the protective effect of TAT-M9 by analyzing $gp91^{phox}$ and $p47^{phox}$ expression. To examine further the important role of NADPH oxidase in the protective effect of TAT-M9, we performed experiments using apocynin, a classic inhibitor of NADPH oxidase. Apocynin protected cells against OGD damage in MTT, LDH release, and ROS generation assays, consistent with the findings of a previous study (Jackman et al. 2009; Lu et al. 2012). We also added TBCA, a novel regulator of NADPH oxidase, to the cultural medium, and found that it reversed the protective effect of TAT-M9. This indicated that the anti-oxidative effect of TAT-M9 may be mediated, at least partially, through the suppression of NADPH oxidase. However, TBCA was shown to enhance the cell damage caused by OGD and to affect the shapes and cytoskeletons of some cell types (Kim et al. 2009; Kramerov et al. 2011). This indicated that the protective effect of TAT-M9 might not be reversed by TBCA, but only weakened following severe injury. However, we did find that TAT-M9 could alter the expression of NADPH oxidase. Thus, to confirm the exact mechanism underlying the effect of TAT-M9, other experiments should be performed.

Nogo-A has long been understood as a principal inhibitor of neurite outgrowth (Wang et al. 2008). Many scientists have proved that Nogo-A blockage could enhance axonal regeneration and improve neuronal damage prognosis. Our result may seem paradox with all these previous studies. However, a recent study proved that the expression of Nogo-A peaked high at 28 days after onset of MCAO, but decreased at the early phase after the injury (Cheatwood et al. 2008). Meanwhile, Nogo-A deficiency mice was more vulnerable to ischemia injury compared with wild-type mice (Kilic et al. 2010). Together with our current results, it indicated that interfering Nogo-A at various time points might result different effects.

In the current study, the mouse HT22 hippocampal cell line was used as model. It is a subclone of the HT4 cell line that was characterized by its sensitivity to oxidative stress (Morimoto and Koshland 1990). As these cells are devoid of ionotropic glutamate receptors, excitotoxicity does not affect HT22 cell death (Davis and Maher 1994). HT22 cell line has been used in many injury models such as glutamate exposure (Yang et al. 2012) and OGD (Jamarkattel-Pandit et al. 2010; Ryou et al. 2012). Currently, we proved that TAT-M9 at certain concentration was effective for OGD injury in HT22 cells. However, cell line is not the first option for studying the OGD effect due to its characteristics. Moreover, even drugs that were effective in vitro could easily fail in vivo. Further study is urgent needed for examining TAT-M9 on cerebral ischemia injury model.

In conclusion, our study confirmed that an HIV-TAT-derived peptide fused to a novel region comprising residues 290–562 of Nogo-A, which could be directly transduced

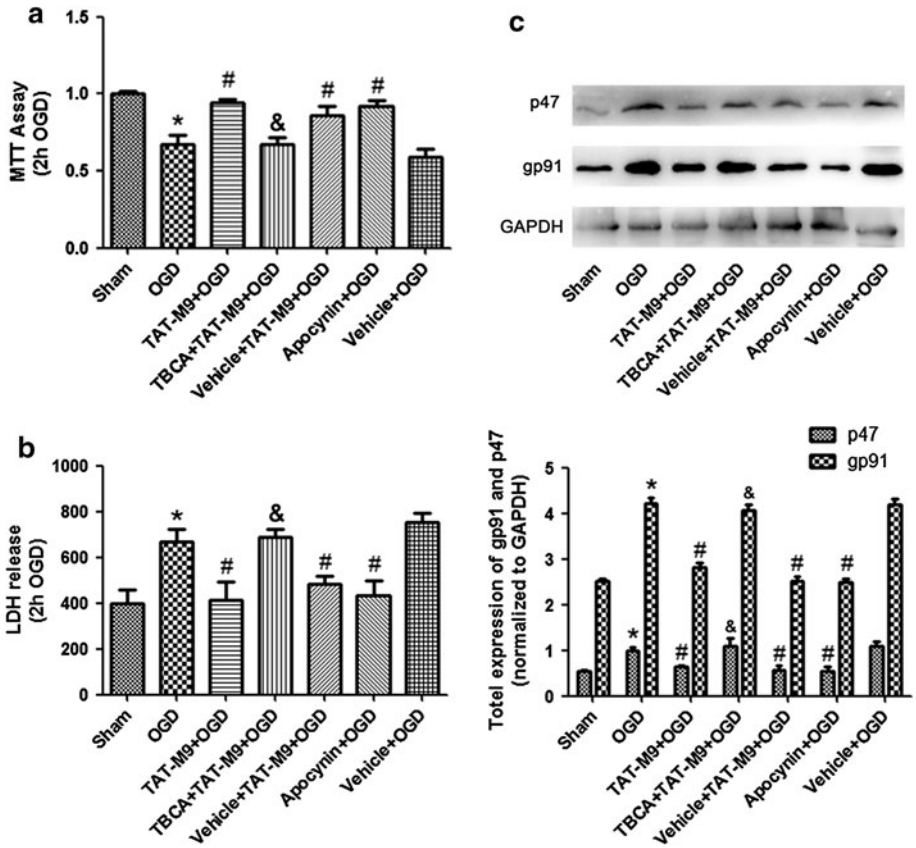

Fig. 5 Involvement of NADPH oxidase in the cytoprotective effect of TAT-M9 in HT22 cells exposed to OGD. **a** Cell viability. TAT-M9 and apocynin improved cell viability. The reduction in cell death by TAT-M9 was reversed by pretreatment with TBCA at a concentration of 10 μmol/L. Values are expressed as mean ± SEM of five per group. $^{*}P < 0.05$ versus OGD group, $^{\#}P < 0.05$ versus TAT-M9 + OGD group. **b** LDH release. TAT-M9 or apocynin treatment markedly attenuated LDH release, whereas the protective effect of TAT-M9 was reversed by pretreatment with TBCA. Values are expressed as mean ± SEM of five per group. $^{*}P < 0.05$ versus OGD group, $^{\#}P < 0.05$ versus TAT-M9 + OGD group. **c** Activation of NADPH oxidase by western blotting of total $gp91^{phox}$ and $p47^{phox}$ (up) and analyses (down) Data are expressed as mean ± SEM of three per group. $^{*}P < 0.05$ versus Sham group, $^{\#}P < 0.05$ versus OGD group, $^{\&}P < 0.05$ versus TAT-M9 + OGD group

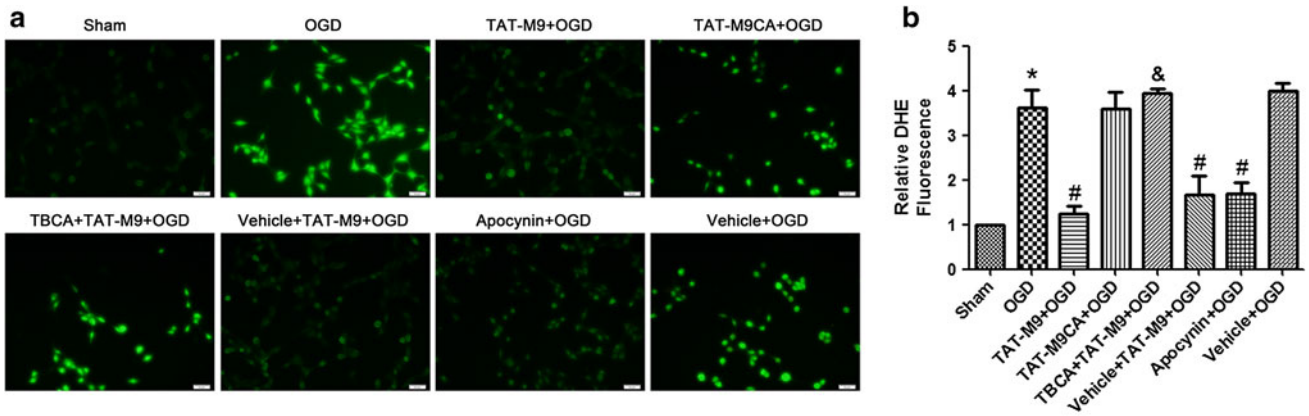

Fig. 6 Effect of TAT-M9 on intracellular ROS levels in HT22 cells exposed to OGD TAT-M9 (0.4 μM) was added to the HT22 neuron cultures during OGD/R. **a** ROS level was examined using DHE under a fluorescence microscope. A strong fluorescence signal was detected in the OGD group. TAT-M9, as well as apocynin, could efficiently reduce ROS production, while TBCA could reverse the protective effect of TAT-M9. **b** Statistical analysis of the relative fluorescence levels in different groups. Values are expressed as mean ± SEM of three per group. $^{*}P < 0.05$ versus Sham group, $^{\#}P < 0.05$ versus OGD group, $^{\&}P < 0.05$ versus TAT-M9 + OGD group

into HT22 cells, exerted neuroprotective effects in an in vitro model of OGD. It protected HT22 cells from apoptosis and inhibited oxidative stress through the suppression of NADPH oxidase. These findings suggest that the TAT-M9 protein may be an efficient therapeutic agent for neuroprotection.

Acknowledgments This work was supported by the Major Program of National Natural Science Foundation of China (Grant 30930091), the Program for Changjiang Scholars and Innovative Research Team in University (Beijing, China, Grant 2010CXTD01), and the National Natural Science Foundation of China (Grants 81072888, 81071060, 81035375).

Conflict of interest The authors declare no conflict of interest.

References

Albrecht J, Hanganu IL, Heck N, Luhmann HJ (2005) Oxygen and glucose deprivation induces major dysfunction in the somatosensory cortex of the newborn rat. Eur J Neurosci 22:2295–2305

Anthony DC, Ferguson B, Matyzak MK, Miller KM, Esiri MM, Perry VH (1997) Differentialmatrixmetalloproteinase expression in cases of multiple sclerosis and stroke. Neuropathol Appl Neurobiol 23:406–415

Bedard K, Krause KH (2007) The NOX family of ROS-generating NADPH oxidases: physiology and pathophysiology. Physiol Rev 87:245–313

Cheatwood JL, Emerick AJ, Schwab ME, Kartje GL (2008) Nogo-A expression after focal ischemic stroke in the adult rat. Stroke 39:2091–2098

Chen H, Song YS, Chan PH (2009) Inhibition of NADPH oxidase is neuroprotective after ischemia–reperfusion. J Cereb Blood Flow Metab 29:1262–1272

Chrissobolis S, Faraci FM (2008) The role of oxidative stress and NADPH oxidase in cerebrovascular disease. Trends Mol Med 14:495–502

Davis JB, Maher P (1994) Protein kinase C activation inhibits glutamate-induced cytotoxicity in a neuronal cell line. Brain Res 652:169–173

Fordel E, Thijs L, Martinet W, Schrijvers D, Moens L, Dewilde S (2007) Anoxia or oxygen and glucose deprivation in SH-SY5Y cells: a step closer to the unraveling of neuroglobin and cytoglobin functions. Gene 398:114–122

Gou X, Wang Q, Yang Q, Xu L, Xiong L (2011) TAT-NEP1-40 as a novel therapeutic candidate for axonal regeneration and functional recovery after stroke. J Drug Target 19:86–95

Jackman KA, Miller AA, De Silva TM, Crack PJ, Drummond GR, Sobey CG (2009) Reduction of cerebral infarct volume by apocynin requires pretreatment and is absent in Nox2-deficient mice. Br J Pharmacol 156:680–688

Jamarkattel-Pandit N, Pandit NR, Kim MY, Park SH, Kim KS, Choi H et al (2010) Neuroprotective effect of defatted sesame seeds extract against in vitro and in vivo ischemic neuronal damage. Planta Med 76:20–26

Katsura K, Takahashi K, Asoh S, Watanabe M, Sakurazawa M, Ohsawa I et al (2008) Combination therapy with transductive anti-death FNK protein and FK506 ameliorates brain damage with focal transient ischemia in rat. J Neurochem 106:258–270

Kemp M, Go YM, Jones DP (2008) Nonequilibrium thermodynamics of thiol/disulfide redox systems: a perspective on redox systems biology. Free Radic Biol Med 44:921–937

Kilic U, Kilic E, Dietz GP, Bahr M (2003) Intravenous TAT-GDNF is protective after focal cerebral ischemia in mice. Stroke 34:1304–1310

Kilic E, ElAli A, Kilic U, Guo Z, Ugur M, Uslu U et al (2010) Role of Nogo-A in neuronal survival in the reperfused ischemic brain. J Cereb Blood Flow Metab 30:969–984

Kim GS, Jung JE, Niizuma K, Chan PH (2009) CK2 is a novel negative regulator of NADPH oxidase and a neuroprotectant in mice after cerebral ischemia. J Neurosci 29:14779–14789

Kramerov AA, Golub AG, Bdzhola VG, Yarmoluk SM, Ahmed K, Bretner M, Ljubimov AV (2011) Treatment of cultured human astrocytes and vascular endothelial cells with protein kinase CK2 inhibitors induces early changes in cell shape and cytoskeleton. Mol Cell Biochem 349:125–137

Krantic S, Mechawar N, Reix S, Quirion R (2007) Apoptosis-inducing factor: a matter of neuron life and death. Prog Neurobiol 81:179–196

Lu Q, Wainwright MS, Harris VA et al (2012) Increased NADPH oxidase-derived superoxide is involved in the neuronal cell death induced by hypoxia–ischemia in neonatal hippocampal slice cultures. Free Radic Biol Med 53:1139–1151

Mi YJ, Hou B, Liao QM, Ma Y, Luo Q, Dai YK et al (2012) Amino-Nogo-A antagonizes reactive oxygen species generation and protects immature primary cortical neurons from oxidative toxicity. Cell Death Differ 10:1038–1050

Miller AA, Dusting GJ, Roulston CL, Sobey CG (2006) NADPH-oxidase activity is elevated in penumbral and non-ischemic cerebral arteries following stroke. Brain Res 1111:111–116

Morimoto BH, Koshland DE Jr (1990) Induction and expression of long- and short-term neurosecretory potentiation in a neural cell line. Neuron 5:875–880

Nagasawa K, Kakuda T, Higashi Y, Fujimoto S (2007) Possible involvement of 12-lipoxygenase activation in glucose-deprivation/reload-treated neurons. Neurosci Lett 429:120–125

Nagel F, Falkenburger BH, Tonges L, Kowsky S, Poppelmeyer C, Schulz JB et al (2008) Tat-Hsp70 protects dopaminergic neurons in midbrain cultures and in the substantia nigra inmodels of Parkinson's disease. J Neurochem 105:853–864

Papadopoulos CM, Tsai SY, Alsbiei T, O'Brien TE, Schwab ME, Kartje GL (2002) Functional recovery and neuroanatomical plasticity following middle cerebral artery occlusion and IN-1 antibody treatment in the adult rat. AnnNeurol 51:433–441

Ryou MG, Liu R, Ren M, Sun J, Mallet RT, Yang SH (2012) Pyruvate protects the brain against ischemia–reperfusion injury by activating the erythropoietin signaling pathway. Stroke 43:1101–1107

Seymour AB, Andrews EM, Tsai SY, Markus TM, Bollnow MR, Brenneman MM et al (2005) Delayed treatment with monoclonal antibody IN-1 1 week after stroke results in recovery of function and corticorubral plasticity in adult rats. J Cereb Blood Flow Metab 25:1366–1375

Susnow N, Zeng L, Margineantu D, Hockenbery DM (2009) Bcl-2 family proteins as regulators of oxidative stress. Semin Cancer Biol 19:42–49

Taylor CP, Burke SP, Weber ML (1995) Hippocampal slices: glutamate overflow and cellular damage from ischemia are reduced by sodium-channel blockade. J Neurosci Methods 59:121–128

Valko M, Leibfritz D, Moncol J, Cronin MT, Mazur M, Telser J (2007) Free radicals and antioxidants in normal physiological functions and human disease. Int J Biochem Cell Biol 39:44–84

Walder CE, Green SP, Darbonne WC, Mathias J, Rae J, Dinauer MC, Curnutte JT, Thomas GR (1997) Ischemic stroke injury is reduced in mice lacking a functional NADPH oxidase. Stroke 28:2252–2258

Wang Q, Gou X, Xiong L, Jin W, Chen S, Hou L, Xu L (2008) Trans-activator of transcription-mediated delivery of NEP1-40 protein

into brain has a neuroprotective effect against focal cerebral ischemic injury via inhibition of neuronal apoptosis. Anesthesiology 108:1071–1080

Yang EJ, Min JS, Ku HY, Choi HS, Park MK, Kim MK et al (2012) Isoliquiritigenin isolated from *Glycyrrhiza uralensis* protects neuronal cells against glutamate-induced mitochondrial dysfunction. Biochem Biophys Res Commun 421:658–664

Yoo BK, Choi JW, Han BH, Kim WK, Kim HC, Ko KH (2005) Role of MAPK/ERK1/2 in the glucose deprivation-induced death in immunostimulated astroglia. Neurosci Lett 376:171–176

Yoshioka H, Niizuma K, Katsu M, Okami N, Sakata H, Kim GS et al (2011) NADPH oxidase mediates striatal neuronal injury after transient global cerebral ischemia. J Cereb Blood Flow Metab 31:868–880